Liquid Crystals
Publication details, including instructions for authors and subscription information:
http://www.informaworld.com/smpp/title~content=t713926090

Chirality in liquid crystals. The remarkable phenylpropiolates

J. W. Goodby[a]; I. Nishiyama[a]; A. J. Slaney[a]; C. J. Booth[a]; K. J. Toyne[a]
[a] The School of Chemistry, The University of Hull, Hull, England

To cite this Article Goodby, J. W. , Nishiyama, I. , Slaney, A. J. , Booth, C. J. and Toyne, K. J.(1993) 'Chirality in liquid crystals. The remarkable phenylpropiolates', Liquid Crystals, 14: 1, 37 — 66
To link to this Article: DOI: 10.1080/02678299308027303
URL: http://dx.doi.org/10.1080/02678299308027303

LIQUID CRYSTALS, 1993, VOL. 14, NO. 1, 37–66

Invited Lecture

Chirality in liquid crystals
The remarkable phenylpropiolates

by J. W. GOODBY*, I. NISHIYAMA, A. J. SLANEY,
C. J. BOOTH and K. J. TOYNE
The School of Chemistry, The University of Hull, Hull HU6 7RX, England

The biphenylyl esters of the 4-*n*-alkoxyphenylpropiolic acids are a unique family of liquid-crystalline materials. In particular, when the biphenyl moiety of the compounds carries a chiral end-group, many optically active mesophases are created which exhibit unusual structures and physical properties. For instance, when the chiral group attached to the biphenyl moiety is 1-methylheptyl then Abrikosov, twist grain boundary smectic A* and antiferroelectric smectic C* phases are observed. The wide variety of chiral phases and electrochiral properties exhibited by this family of materials makes them ideal candidates for exploring chirality in the liquid-crystalline state. These investigations allow us to contrast and compare chirality dependent phenomena in liquid crystals, thereby producing a broader view of the concept of chirality in organized fluids than is traditionally presented.

1. Introduction

The concept of chirality has a unique position in the history of liquid crystals. The first thermotropic liquid crystal to be discovered [1], over 100 years ago, was in fact a cholesteric mesophase exhibited by an optically active derivative of cholesterol. Although being present in the first discovered thermotropic mesophase, it is only in the past 20 to 30 years that chirality in liquid crystal systems has taken on many different guises. Today chirality in ordered fluids is, indirectly, one of the most studied branches of the field of liquid crystals.

1.1. *Cholesteric and blue phases*

Initially great interest was shown in cholesteric mesophases, particularly when it was found that their property of selectively reflecting light could be exploited in thermochromic applications, such as in thermometers [2]. In the cholesteric phase the lath-like molecules, which possess asymmetric structures pack, so as to create a helical macrostructure in a direction perpendicular to their long axes. This macrostructure is itself optically active and so the mesophase also exhibits form optical activity along with the typical molecular optical activity that would be found for a normal liquid.

At about the same time that research into thermochromism was taking place, detailed studies of the optical changes which occur at the clearing point to the isotropic

* Author for correspondence.

0267–8292/93 $10·00

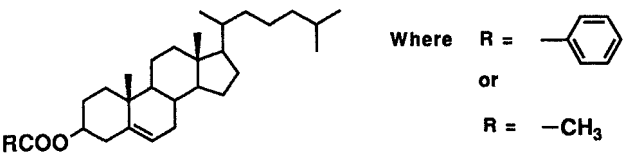

Figure 1. Structures of the first liquid crystal materials.

liquid revealed that yet another set of unique chiral mesophases exists—the so-called blue phases. These phases have extraordinary frustrated double twist structures which have been the subject of many physical studies since their original discovery in 1973 [3]. However, it is possibly safe to say that, even though many excellent studies on the elucidation of their structures have been performed, the full details of their structures are yet to emerge [4].

1.2. *Ferroelectric and chiral smectic C* phases*

In the mid 1970s the topic of chirality in liquid crystals shifted into the world of smectic liquid crystals, and in particular into the realm of the smectic C phase, which has C_{2h} symmetry. It had been known for a very long time that when this phase is composed of optically active molecules it usually exhibits a helical macrostructure, similar in nature to that of the cholesteric phase. Thus, the mesophase also exhibits form optical activity. The helical structure is based on the rotation of the tilt direction of individual layers of the phase about an axis normal to the layer planes on passing from layer to layer. Consequently, the phase itself is optically active and can selectively reflect light when the pitch of the helical structure is comparable to the wavelength of light. Thus, the mesophase was given the miscibility coding of smectic C*. Later Meyer [5] predicted that when a smectic C phase is composed of chiral molecules, its space symmetry is reduced to C_2, as shown in figure 2, and therefore it will exhibit ferroelectric properties. The subsequent invention of a fast switching light valve, based on the properties of ferroelectric liquid crystals, by Clark and Lagerwall [6] led to an explosion of interest in ferroelectric liquid crystals and their chiral properties for the purposes of exploitation in display applications. This proved to be a remarkable sequence of events, considering that the first smectic C* materials date back to the 1920s.

1.3. *Electroclinism*

After the discovery of the first ferroelectric smectic C* material by Meyer and co-workers [7], Meyer and Garoff [8] went further to show that the smectic A phase could also have a reduced D_∞ symmetry (from $D_{\infty h}$) which was manifested through a new electrochiral effect that they called electroclinism. Again this property is the subject of intense studies for applications in optical communications and optical networking. Apart from the chiral smectic A* phase, other chiral orthogonal phases, notably the crystal B* and crystal E* phases, were also shown to exhibit electroclinic properties in a way similar to that in the smectic A* phase, but in the case of the crystal phases the effects were found to be not as pronounced [9].

Current interest in chiral smectic liquid crystals has centred around two new exciting and differing phenomena; those of antiferrolectric and ferrielectric phases and twist grain boundary (TGB) structures.

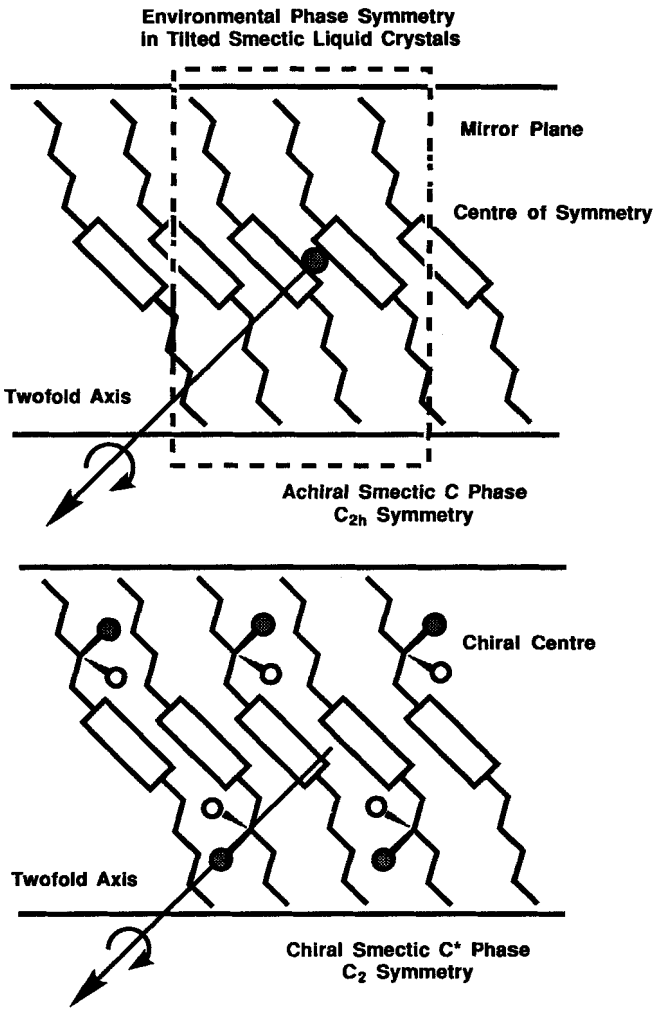

Figure 2. Symmetry in the smectic C and smectic C* phases. (Note the molecules are in dynamic motion).

1.4. *Ferrielectric and antiferroelectric phases*

Antiferroelectric properties in liquid crystal systems were discovered only 3 years ago [10], however, in this time it has already been demonstrated that antiferroelectric smectic C* materials can be utilized in fast switching display device applications [11]. The antiferroelectric and ferrielectric smectic C* phases have the general structure shown in figure 3, where the molecules are tilted in opposite directions in adjacent layers. For the antiferroelectric phase there are an equal number of oppositely tilted layers, whereas for the ferri-phase the distribution is unequal. As a consequence of this ordering the spontaneous polarization is averaged to zero for the bulk unwound antiferro-phase in a zero electric field, but for the ferri-phase there is a residual spontaneous polarization. Materials that have the antiferroelectric phase structure and related properties have an advantage over conventional ferroelectric smectic C* materials in that they exhibit well-defined electrical field thresholds for switching [12], and hence, in principle, they should be easier to multiplex. The sharper field threshold is

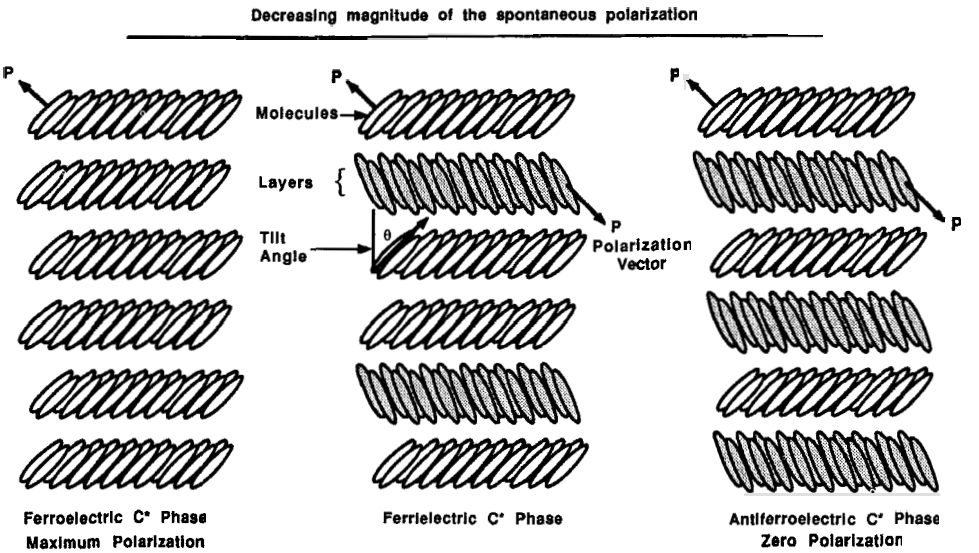

Figure 3. Structure of the ferroelectric, ferrielectric, and antiferroelectric phases.

a consequence of switching that takes place from the antiferroelectric phase to the ferroelectric phase; the contrast in the display being derived from fields of opposite polarity.

1.5. *Twist grain boundary phases*

In 1972 de Gennes [13] predicted that, at a second order nematic to smectic A phase transition, a defect stabilized intermediary phase could occur when the liquid crystal was subjected to twist or bend distortions. Thus, at this transition strong fluctuations from neighbouring phases are felt. Therefore, an intermediary phase can be stabilized at the S_A–N transition in a mechanically stressed liquid crystal. He drew an analogy between the physical nature of such phase behaviour and that of transitions in superconductors. De Gennes suggested that twist and bend distortions can be incorporated into a layered smectic A structure *via* the presence of an array of screw or edge dislocations. The screw dislocations permeate the normal smectic A phase to produce a lattice, and in his analogy this is similar to how the conducting phase permeates the superconducting phase to form a lattice of vortices in the Abrikosov phase of Type II superconductors. Points concerning the de Gennes analogy between superconductors and liquid crystal phases are summarized in table 1.

De Gennes' arguments were further developed by Renn and Lubensky [14] who suggested that such an intermediary phase could be formed at the cholesteric to smectic A* transition and stabilized by screw dislocations. They called this phase the twist grain boundary phase (TGB_A^*). Thus, at a normal cholesteric to smectic A* transition, the helical ordering of the cholesteric phase gives way to the formation of the layered structure of the smectic A* phase. However, for a transition mediated by such an intermediary phase, the molecules try to form a helical structure, where the axis of the helix is perpendicular to the long axes of the molecules (as in the cholesteric phase), yet at the same time the molecules also wish to form the lamellar structure of the smectic A* phase (see figure 4). These two structures are incompatible and cannot co-exist and fill space uniformly without forming defects. The matter is resolved by the formation of a

Table 1. The de Gennes analogy between superconductors and liquid crystals (after Renn and Lubensky).

The de Gennes analogy	
Superconductor	Liquid crystal
ψ = Cooper pair amplitude	ψ = density wave amplitude
$\mathbf{A}$ = vector potential	$\mathbf{n}$ = nematic director
$\mathbf{B} = \nabla \times \mathbf{A}$ = magnetic induction	$\mathbf{k}_0 = \mathbf{n} \cdot \nabla \times \mathbf{n}$ = twist
Normal metal	Nematic phase
Normal metal in a magnetic field	Cholesteric (N*) phase
Meissner phase	Smectic A phase
Meissner effect	Twist expulsion
London penetration depth λ	Twist penetration depth λ_t
Superconducting coherence length ξ	Smectic correlation length ξ
Vortex (magnetic flux tube)	Screw dislocation
Abrikosov flux lattice	Twist grain boundary phase

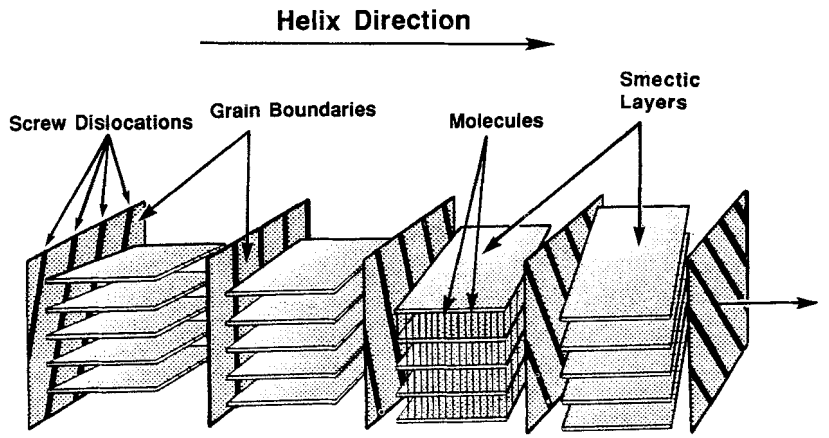

Figure 4. Structure of the Abrikosov TGB_{A^*} phase.

lattice of screw dislocations which enables a quasi-helical structure to co-exist with a layered structure. This is achieved by having small blocks of molecules, that have a smectic A structure, being rotated with respect to one another, thereby forming a helical structure. The blocks are separated from one another by screw dislocations. This type of defect allows the blocks to be rotated through a small angle with respect to one another. As a helix is formed with the aid of screw dislocations, the dislocations themselves are periodic. It is predicted that rows of screw dislocations will form grain boundaries in the phase and hence the new phase was referred to as the twist grain boundary (TGB) phase. The structure of the twisted smectic A* (TGB) phase is shown in figure 4.

Examples of this theoretically predicted phase were first found in some propiolate esters [15] of high liquid-crystalline chirality. Certain members of this family of materials exhibit exotic phase behaviour in that they form the twist grain boundary phase directly on cooling from the isotropic liquid. The helical structure in the TGB_{A^*} phase appears from experiments to have a pitch length in the range of 0·38 to 0·63 μm, and therefore the phase, like the cholesteric phase, selectively reflects light. Studies

appear to indicate that the block size is about 185 Å, which is quite small considering that the phase is still smectic [16]. Thus, these remarkable phases and phase transitions are products of the competition between chirality and conventional phase structure.

It is thought that the defects in the phase might be stabilized by impurities in the material. In the case of chemically pure compounds, the impurity could be due to the presence of the minority enantiomer in materials where the enantiomeric excess is less than 100 per cent. Thus, the enantiomer present in the lesser amount could migrate to the cores of the defects, thereby stabilizing them by the formation of a nematic phase in the centres of the cores. This suggests that these frustrated phases (blue phases and Abrikosov phases) are inhomogeneous in the distribution of their enantiomeric components. This hypothesis is supported by indications from experimental studies that the greater the optical purity of the compound, the shorter the temperature range of the frustrated phase becomes [17].

Abrikosov-like phases have also been detected in optically active side chain liquid crystal polymers [18]. When the polymer forms a liquid crystal phase it is thought that the main chain of the polymer prevents a cholesteric phase from forming and instead induces the formation of a smectic A phase. However, the strong chirality of the side group forces the layers to twist to give an Abrikosov phase.

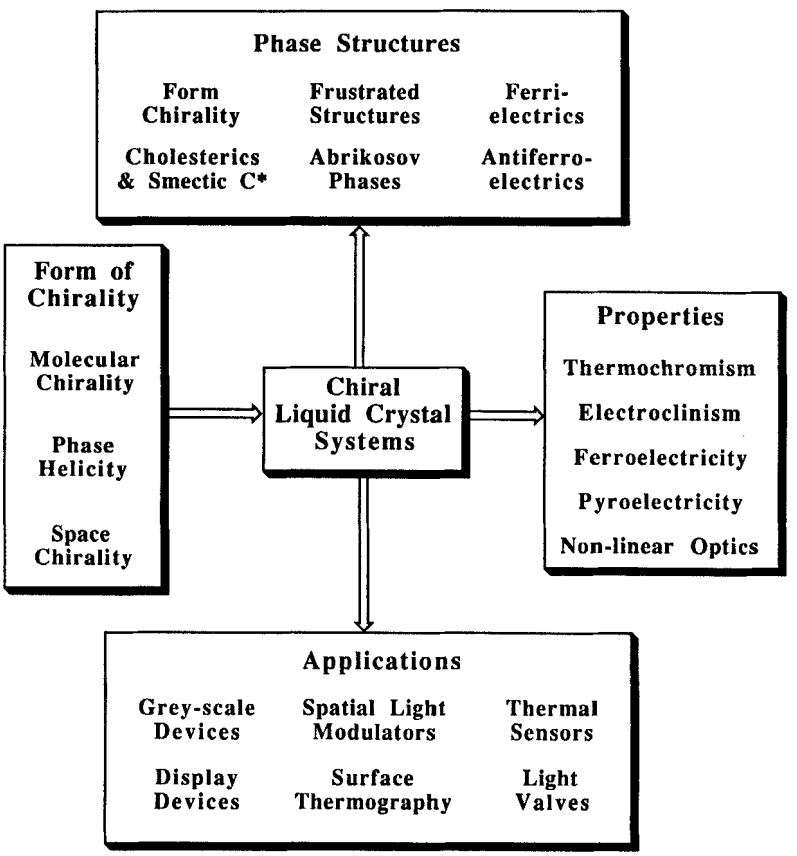

Figure 5. Schematic representation of the relationship between chirality and liquid-crystallinity.

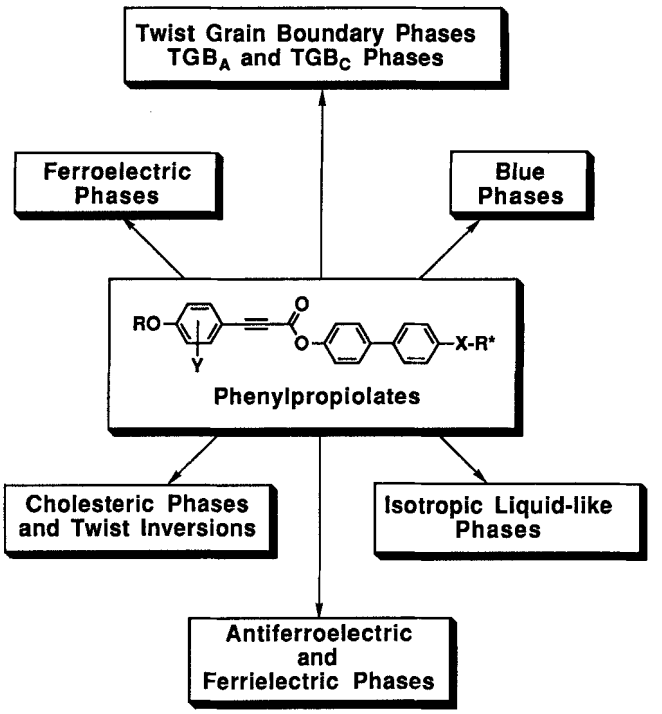

Figure 6. Properties of phenylpropiolates.

Generally, many chiral liquid crystal properties are closely related, and figure 5 is an attempt to show a schematic representation of the relationship between phase and molecular chirality and phase structure, physical properties, and applications of chiral liquid crystals. Our current work on chirality in liquid crystals [19, 20] has involved the investigation of the effect of molecular chirality on the incidence and properties of chiral liquid crystal mesophases, such as Abrikosov twist grain boundary phases [9], blue phases, and ferroelectric, antiferroelectric, and ferrielectric phases [10]. We have found that optically active derivatives of the 4-*n*-alkoxyphenylpropiolic acids are unique in that they are capable of exhibiting many of these phases and are therefore ideal candidates for model studies on the effect of chirality in liquid crystals. Figure 6 shows a typical structure of the phenylpropiolate esters that were prepared and investigated. From this family of materials twist grain boundary phases, blue phases, and ferroelectric, antiferroelectric, ferrielectric, electroclinic, and cholesteric phases were obtained. These materials also have unique properties in that they show unusual isotropic to isotropic liquid transitions, twist inversions in helical phases, and twist grain boundary smectic C* phases. In the following Results and discussion section, the properties of some novel phenylpropiolates will be described.

2. Results and discussion

2.1. *Material structure*

A variety of derivatives of the 4-*n*-alkoxyphenylpropiolic acids have been prepared over the last 3 to 4 years by both the groups at AT&T Bell Laboratories and Hull University. Compounds of the general structure shown in figure 7 have been synthesized and their physical properties investigated [21]. For aliphatic terminal

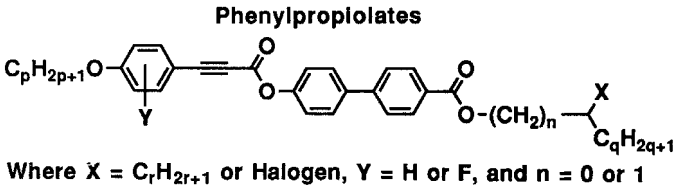

Figure 7. General structures of phenylpropiolates.

groups (p, q, r), the independent variation of the lengths of the two aliphatic chains, denoted by C_qH_{2q+1} and C_rH_{2r+1}, alters the chirality of the system. For example, for a value of $r = 1$, lengthening of the other alkyl chain, by increasing the value of q from 2 to 6, increases the chirality of the system (for a constant value of, say, 10 for the *n*-alkoxy chain length, p). The increasing degree of the chirality can be inferred from a rising value of the spontaneous polarization and a decrease in the pitch of the macroscopic helical structure in the ferroelectric smectic C* phase as the value of q is increased (for example, for constant values of $p = 10, r = 1$). Similarly, we find that when the length, r, of the off-axis alkyl substituent is increased the incidence of antiferroelectric phases also increases. In both cases, we believe that, by increasing the alkyl chain lengths, q and r, the molecular rotation which occurs about the chiral centre becomes progressively more damped in systems such as the smectic C* phase. This is because the rotation will induce higher energy changes in the system; consequently the chirality becomes higher. Similarly, we have investigated the liquid-crystalline properties of materials where the polarity at the chiral centre is varied. This was achieved by positioning a halogen atom in a lateral position at the chiral centre relative to the long axis of the molecule. Thus we were able to examine chiral properties as a function of polarity as well as steric shape.

2.2. *General synthesis of phenylpropiolates*

Phenylpropiolates are typically prepared by the synthetic pathway shown in figure 8. The 4-*n*-alkoxyphenylpropiolate portion of the target compound is prepared from 4-hydroxybenzaldehyde, **1**, which is alkylated with a suitable *n*-alkylbromide in the presence of anhydrous potassium carbonate. The resulting, *n*-alkoxybenzaldehyde, **2**, is then converted into the analogous β,β-dibromostyrene, **3**, by the use of a mixture of carbon tetrabromide, zinc and triphenylphosphine. Butyl lithium dehydrobrominates the styrene to give the corresponding lithium acetylide which with solid carbon dioxide and work-up under acid conditions generates the free 4-*n*-alkoxyphenylpropiolic acid, **4** [22]. The biphenyl portion of the target material is prepared starting from 4-methoxy-4′-cyanobiphenyl, **5**. This compound is hydrolysed and demethylated in one step using aqueous hydrobromic acid (48% wt/vol) in glacial acetic acid. The product, 4′-hydroxybiphenyl-4-carboxylic acid, **6**, is protected with methyl chloroformate at 0°C to give 4-methoxycarbonyloxybiphenyl-4-carboxylic acid, **7**. This carboxylic acid is esterified with an appropriate alcohol in the presence of triphenylphosphine and diethyl azodicarboxylate (DEAD) [23] which avoids deprotection of **7**. The carbonate ester produced, **8**, is converted into the corresponding biphenol ester, **9**, by removal of the carbonate protecting group by stirring at room temperature in ethanolic ammonia solution [24]. The resulting chiral 4′-hydroxybiphenyl-4-carboxylate, **9**, is then esterified with the 4-*n*-alkoxyphenylpropiolic acid in the presence of dicyclohexylcarbodiimide (DCC) and *N*,*N*-dimethylaminopyridine (DMAP) [25], to give the alkyl 4′-(4″-*n*-alkoxyphenylpropioloyloxy)biphenyl-4-carboxylate, **10**.

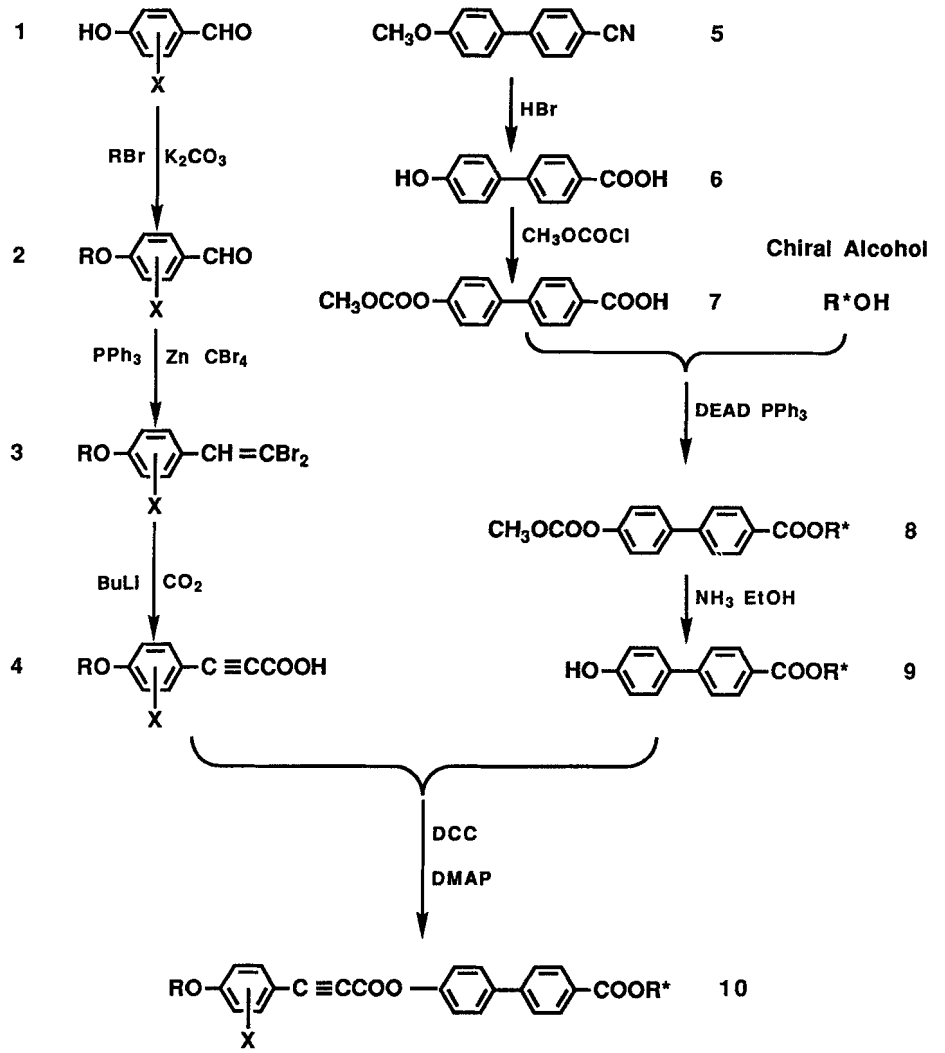

Figure 8. General synthesis of the phenylpropiolates.

2.3. *Twist grain boundary phases*

2.3.1. *The (R)- and (S)-1-methylheptyl esters*

The first twist grain boundary phases found in low molar mass materials were discovered in the (*R*)- and (*S*)-1-methylheptyl 4′-(4″-*n*-alkoxyphenyl-propioloyloxy)biphenyl-4-carboxylates (1M7*p*OPPBCs); the general chemical structure for this family is shown in figure 9. The phase transitions for this series were determined by both thermal optical microscopy and differential scanning calorimetry; the results (omitting the melting points) are shown in table 2. The transition temperatures for the series are plotted as a function of increasing alkoxy chain length in figure 10. It can be seen from this figure that, as the terminal alkoxy chain increases in length, the smectic A* to smectic C* transition temperatures rise sharply. Over the same interval of chain length the smectic A* to isotropic liquid transition temperatures

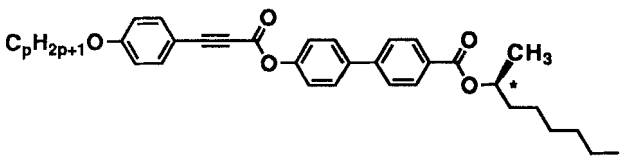

Figure 9. (*R*)- and (*S*)-1-methylheptyl 4′-(4″-*n*-alkoxyphenylpropioloyloxy)biphenyl-4-carboxylates (1M7*p*OPPBCs).

Table 2. Transition temperatures and clearing point enthalpies (kJ mol^{-1}) for the (*R*)- and (*S*)-1-methylheptyl 4′-(4″-*n*-alkoxyphenylpropioloyloxy)biphenyl-4-carboxylates (1M7*p*OPPBCs).

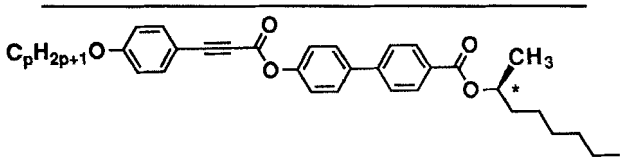

p	Phase behaviour	ΔH_C/kJ mol^{-1}†
8	I 97·5°C S_A^*	3·93
9	I 97·5°C S_A^*	3·43
10	I 98·0°C S_A^* 76·3°C S_C^*	3·69
11	I 95·0°C S_A^* 78·1°C S_C^*	2·21
12	I 96·3°C S_A^* 786·0°C S_C^*	2·39
13	I 94·1°C TGB_{A^*} 88·3°C S_C^*	1·37
14	I 93·8°C TGB_{A^*} 89·7°C S_C^*	0·82
15	I 91·6°C TGB_{A^*} 90·6°C S_C^*	0·76
16	I 99·0°C S_C^*	1·15

† Falling enthalpy values—the transition appears to be becoming second order.

fall, thereby decreasing the temperature range of the smectic A* phase. For the *n*-hexadecyloxy homologue this effect culminates in a direct smectic C* to isotropic liquid transition. Thus, the smectic A* phase for at least the *n*-decyloxy member onwards senses fluctuations from both the isotropic liquid and the smectic C* phase. If we now examine the variation in the clearing point enthalpy with respect to chain length we find that the values fall sharply as the *n*-alkoxy chain length is increased. Thus, the clearing transition appears to become more second order in nature with increasing *n*-alkoxy chain length.The decrease in enthalpy values coupled with the decreasing smectic A* range appear to satisfy the criteria set out by de Gennes for the emergence of dislocation stabilized phases, and hence the tridecyl to pentadecyl homologues were found to exhibit twist boundary smectic A* phases (TGB_{A^*}).

The general experimental observations made on this series of compounds are reported elsewhere [15] and hence are not discussed in detail here. However the list below summarizes the major points found from optical, thermal, and structural studies.

- Short chain, C_8 to C_{12}, homologues exhibit normal smectic A* phases.
- Long *n*-alkoxy chain members (C_{13} to C_{15}) exhibit abnormal optical properties.
- The smectic A* temperature range decreases sharply as the chain length increases.
- The isotropic liquid to smectic A* transition enthalpies fall as the series is ascended.
- The abnormal TGB_{A^*} phase is iridescent and therefore has a helical structure.

- The helical axes in the smectic TGB_{A^*} and smectic C* phases are orthogonal to one another.
- The TGB_{A^*} phase for the C_{13} to C_{15} homologues shows a fingerprint texture, hence the phase is helical.
- X-ray diffraction shows that layers are present in the intermediary TGB_{A^*} phase.
- DSC and X-ray studies show abnormalities in the liquid phase above the liquid crystal state.
- The racemates show normal smectic A and C phases.
- Conclusion—the TGB_{A^*} phase is helical and the helix axis lies in the plane of the layers.
- A further new phase exists in the isotropic liquid which is possibly similar to blue phase III (fog phase).

Possibly the most important observation made from these experiments was that the mesophase formed on cooling the isotropic liquid for the C_{13} to C_{15} homologues was helical. Clearly it could not be a cholesteric phase as the earlier members of the series did not exhibit this phase. On cooling the phase into the smectic C* phase the helical

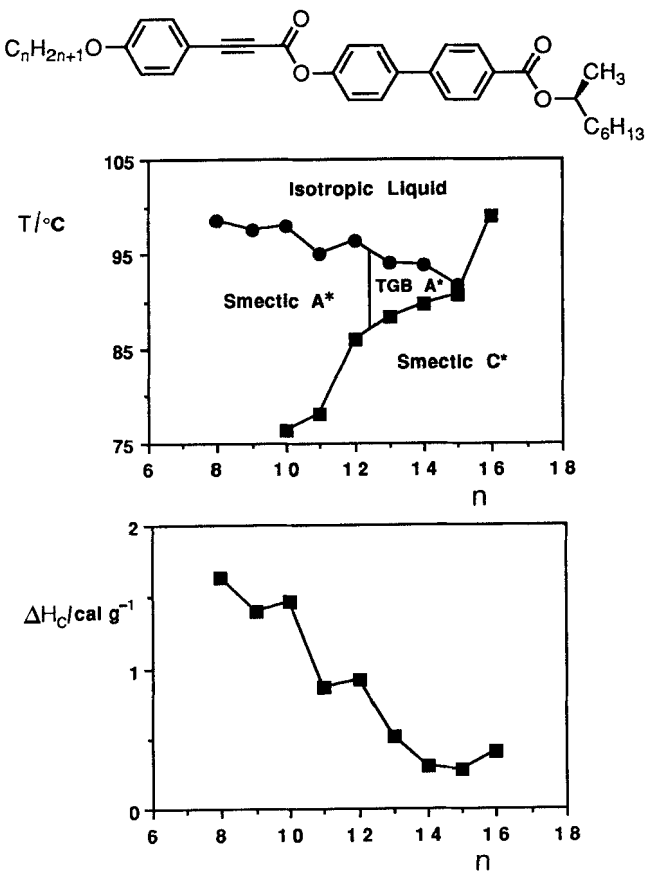

Figure 10. Transition temperatures and clearing point enthalpies as a function of *n*-alkoxy chain length for the (*R*)- and (*S*)-1-methylheptyl 4′-(4″-*n*-alkoxyphenylpropioloyloxy)biphenyl-4-carboxylates (1M7*p*OPPBCs).

axis turned through 180°; thus the helix direction is at right angles in the smectic C* phase with respect to its direction in the intermediary TGB phase. This result can only mean that the helix is in the plane of the layers.

Analysis of the thermal and optical experiments made X-ray diffraction an important tool in verifying that the intermediary TGB phase had a layer structure [16]. This was achieved, but the presence of a lattice of screw dislocations and the pitch of the helix, as predicted by Renn and Lubensky, could not be determined by this method because their periodicity was too great for X-ray analysis to be performed. Recently, however, the presence of a lattice of defects has been investigated by freeze fracture, coupled with light scattering studies on the *n*-tetradecyloxy homologue. The results are fairly conclusive that a lattice exists and that the phase has a helical structure [26].

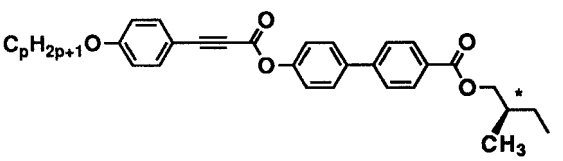

Figure 11. (*S*)-2-methylbutyl 4′-(4″-*n*-alkoxyphenylpropioloyloxy)biphenyl-4-carboxylates (2M4*p*OPPBCs).

Table 3. Transition temperatures and enthalpies for the (*S*)-2-methylbutyl 4′-(4″-*n*-alkoxyphenyl-propioloyloxy)biphenyl-4-carboxylates (2M4*p*OPPBCs).

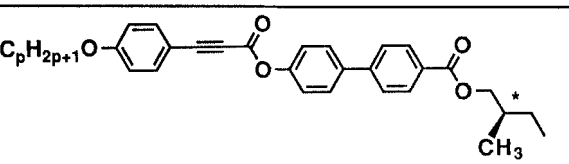

p	mp/°C	T_{Ch}/°C	$T_{ChS_A^*}$/°C	$T_{S_A^*S_C^*}$/°C	T_{Rec}/°C
8	80·1	145·6	108·0	(70·5)	54·5
	[40·9]	[0·13]	[0·16]	[a]	
9	72·2	144·2	116·6	80·5	58·2
	[33·7]	[1·04]	[0·16]	[a]	
10	81·0	142·0	122·5	89·6	69·3
	[36·5]	[0·95]	[0·45]	[a]	
11	80·2	140·8	123·2	94·4	69·4
	[37·7]	[0·95]	[0·41]	[a]	
12	84·0	136·0	125·7	94·0	75·5
	[39·4]	[1·02]	[0·42]	[a]	
13	81·5	132·3	126·0	98·2	70·4
	[39·4]	[1·12]	[0·87]	[a]	
14	76·6	131·0	125·3	98·3	60·8
	[39·0]	[1·07]	[1·28]	[a]	
16	73·7	127·3	127·3	100·9	53·0
	[35·9]	[1·49]	[1·23]	[a]	

( ), monotropic phase; [ ], ΔH values in kJ mol^{-1}; [a], ΔH value too small to be measured.

2.3.2. *The (S)-2-methylbutyl esters*

Further property–structure correlations on various phenylpropiolates proved particularly interesting. The (*S*)-2-methylbutyl 4′-(4″-*n*-alkoxyphenylpropioloyloxy)biphenyl-4-carboxylates were the next set of materials to be investigated [27] (see figure 11), mainly because of the commercial availability of (*S*)-2-methylbutan-1-ol. These materials were found to exhibit smectic A* and smectic C* phases like the analogous 1-methylheptyl esters, but in this case the temperature range of the smectic A* phase did not totally contract on increasing the *n*-alkoxy chain length (*p*). Moreover, on extending the *n*-alkoxy chain the enthalpies for the clearing point transition did not decrease, but increased instead. Thus, the isotropic to smectic A* transition became stronger as the molecular length was increased. This result suggests that the layer ordering also becomes stronger as the series is ascended, and there is a concomitant decrease in the possibility of forming twist grain boundary phases.

The transition temperatures and enthalpies of transition for this series of compounds are given in table 3. In this series the cholesteric phase was found for the earlier homologues, in contrast to the 1-methylheptyl derivatives which did not exhibit cholesteric phases due to the length of the terminal aliphatic chain.

2.3.3. *The (R)- and (S)-1-methylnonyl and 1-methylundecyl esters*

Studies of the effect of extending the terminal aliphatic chain on the peripheral side of the chiral centre were also made [28], through the synthesis and characterization of the (*R*)- and (*S*)-1-methylnonyl and (*R*)- and (*S*)-1-methylundecyl 4′-(4″-*n*-alkoxyphenylpropioloyloxy)biphenyl-4-carboxylates (1M9*p*OPPBCs and 1M11*p*OPPBCs); the general structures for these two families of esters are shown in figure 12. The transition temperatures for these two series are shown together as a function of increasing terminal *n*-alkoxy chain length in figure 13 and listed in table 4 (see later). As with the 1-methylheptyl analogues the smectic C* to smectic A* transition tempera-

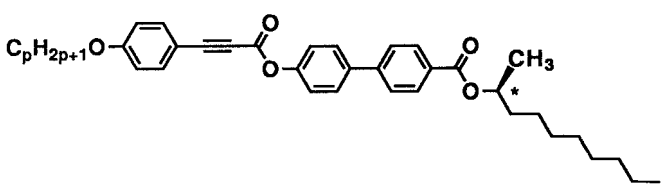

(*R*)- and (*S*)-1-methylnonyl 4′-(4″-*n*-alkoxyphenylpropioloyloxy)biphenyl-4-carboxylates (1M9*p*OPPBCs).

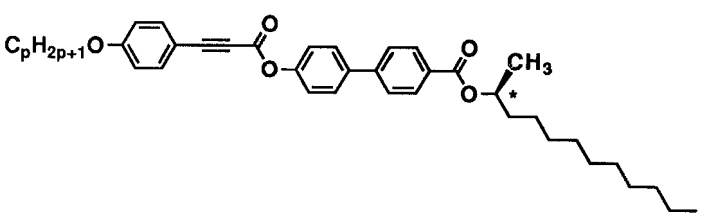

(*R*)- and (*S*)-1-methylundecyl 4′-(4″-*n*-alkoxyphenylpropioloyloxy)biphenyl-4-carboxylates (1M11*p*OPPBCs).

Figure 12.

Table 4. The transition temperatures for the (*R*)- and (*S*)-1-alkylalkyl 4′-(4″-*n*-alkoxyphenylpropioloyloxy)biphenyl-4-carboxylates.

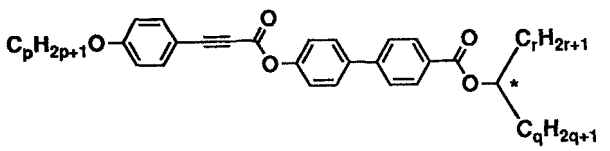

p	*q*	*r*	$T_{ITGB^*_A}$ /°C	$T_{TGB^*_A}$ or $T_{IS^*_A}$ /°C	$T_{S^*_A S^*_C}$ /°C	$T_{S^*_C S^*_C(ferri)}$ /°C	$T_{S^*_C S^*_C(anti)}$ /°C	T_{Rec} /°C	Config.
9	8	1	—	94·8	60·3	—	—	35·0	*S*
12	8	1	—	93·7	83·6	—	—	65·8	*S*
14	8	1	91·0	89·6	89·6	38·6	—	49·8	*R*
16	8	1	—	—	88·0	—	—	42·0	*S*
18	8	1	—	—	86·5	—	—	49·3	*S*
9	10	1	—	94·4	55·0	—	—	42·0	*S*
12	10	1	—	92·8	84·8	—	—	53·8	*S*
14	10	1	89·8	—	89·3	—	—	67·4	*S*
16	10	1	—	—	83·5	—	—	75·1	*S*
18	10	1	—	—	81·1	—	—	49·2	*S*
9	6	2	—	70·8	46·8	—	46·5	<RT†	*S*
12	6	2	—	59·4	56·6	—	55·0	<RT†	*S*
14	6	2	—	—	—	—	—	5·2	*R*
16	6	2	—	—	—	—	—	8·6	*S*
18	6	2	—	—	—	—	—	46·6	*S*
9	6	3	—	62·9	—	—	44·3	<RT†	*R*
12	6	3	—	—	—	—	—	32·8	*R*

† Below room temperature.

tures rise as the series is ascended, whereas the isotropic to smectic A* transitions fall slowly. In both series the smectic A* phase is eclipsed by the smectic C* phase at an alkoxy chain length of 14, the *n*-tetradecyloxy homologue. Thus, in both series the smectic A* TGB phase only appears for the *n*-tetradecyloxy member. Consequently, extending the aliphatic chain on the peripheral side of the chiral centre has the effect of reducing the incidence of TGB_{A^*} phases. This may be due to the fact that when increasing the peripheral chain, the molecular chirality initially increases because the rotation of the chiral centre about the long axis of the molecule becomes increasingly damped. As the peripheral chain is increased in length the effect of rotational damping caused by the addition of extra methylene units will reach a maximum. This effect will then be diluted as the chain is extended further, i.e. as in the case of the 1-methyloctyl and 1-methylundecyl esters.

The differential scanning thermograms for these two series also proved to give very interesting results. Figure 14 shows the cooling thermograms for the *n*-nonyloxy, *n*-dodecyloxy, *n*-tetradecyloxy, *n*-hexadecyloxy, and *n*-octadecyloxy homologues of the 1-methylnonyl series. It can be seen that the trace for the *n*-nonyl member appears relatively normal, but for the *n*-dodecyloxy compound an extra shoulder appears at the isotropic liquid to smectic A* transition, and the smectic A* to smectic C* transition starts to become more first order in nature. As the terminal *n*-alkoxy chain length is increased to fourteen carbon atoms a TGB smectic A* phase appears, the TGB_{A^*} to

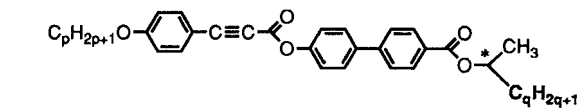

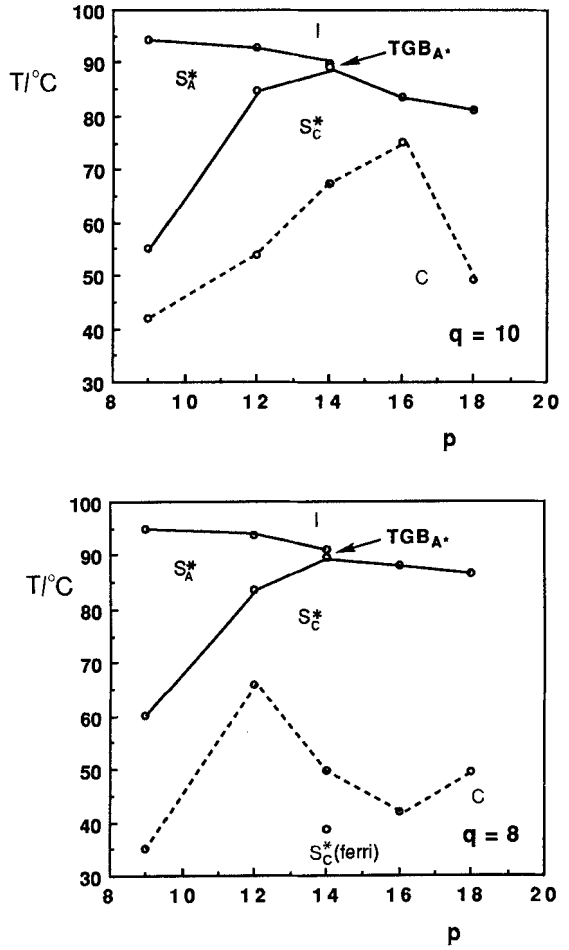

Figure 13. Transition temperatures of the (*R*)- and (*S*)-1-methylnonyl 4′-(4″-*n*-alkoxyphenylpropioloyloxy)biphenyl-4-carboxylates (1M9*p*OPPBCs), and the (*R*)- and (*S*)-1-methylundecyl 4′-(4″-*n*-alkoxyphenylpropioloyloxy)biphenyl-4-carboxylates (1M11*p*OPPBCs) shown as a function of increasing *n*-alkoxy chain length (*p*).

smectic C* transition becomes almost first order, and an isotropic liquid to isotropic liquid transition appears above the transition to the liquid crystal state on cooling. Further chain extension results in the disappearance of the TGB_{A^*} phase which is replaced by a direct transition from the liquid to the smectic C* phase. Again a transition from one liquid phase to another was found above the transition to the liquid-crystalline state. The transitions found in the liquid phase are clearly not artifacts of the instrumental procedure, nor are they due to impurity effects as the qualities of the materials were carefully evaluated by high performance liquid chromatography (all materials were purified to better than 99 per cent chemical purity

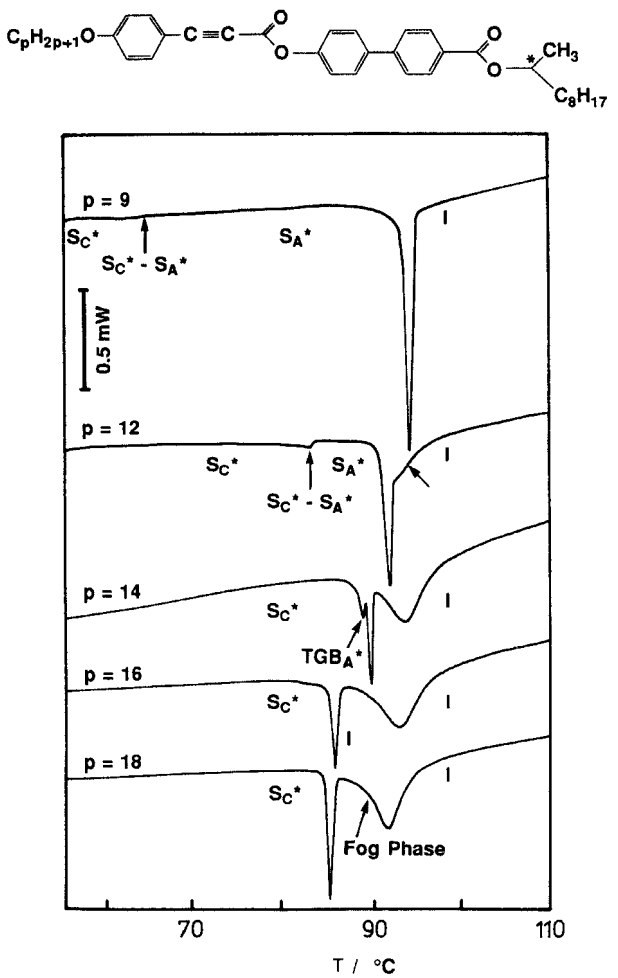

Figure 14. Differential scanning calorimetry (cal g^{-1}) traces for cooling scans (5°C min^{-1}) of the (*R*)-and (*S*)-1-methylnonyl 4′-(4″-*n*-alkoxyphenylpropioloyloxy)biphenyl-4-carboxylates (1M9*p*OPPBCs).

by a combination of flash chromatography and recrystallization). Thus, these materials like their 1-methylheptyl counterparts exhibit transitions in the isotropic liquid phase, but in the case of these two series the transition is also seen to precede the phase change from liquid to smectic C*. The nature of this novel phase behaviour will be discussed later.

Mixture work on these materials also supports de Gennes' contention that the temperature range of the TGB_{A*} phase should be short enough for fluctuations from neighbouring phases to be present. For instance, figure 15 shows a binary phase diagram for mixtures of the *n*-dodecyl and *n*-octadecyloxy members of the 1-methylundecyl series of esters. The *n*-dodecyl member exhibits smectic A* and smectic C* phases, whereas the *n*-octadecyloxy compound only exhibits a smectic C* phase. In the phase diagram, therefore, the temperature range of the smectic A* phase decreases as the proportion of the *n*-octadecyl homologue increases, and a point is reached at about 50 per cent of each component in the mixture where the smectic A* phase is

eclipsed. In the range 30 to 50 per cent of the *n*-octadecyloxy compound in the binary mixture, a TGB_{A^*} phase is observed at the transition from the isotropic liquid crystal state. Thus, in this region the smectic A* phase experiences fluctuations from both the smectic C* phase and the isotropic liquid. These combined effects probably weaken the layers in the phase sufficiently for the twist grain boundary phase to appear.

2.3.4. *Dipolar effects—the polarity of the linking group*

So far, we have only examined alkyl biphenyl esters of the phenyl propiolic acids; in the next section the properties of the chiral alkanoyl esters are presented, where the ester group linking the chiral aliphatic chain to the biphenyl part of the core is replaced by a carbonyl moiety [28]. Thus, the (*S*)-4-(2′-methyloctanoyl)biphenylyl 4-*n*-alkoxyphenylpropiolates (see figure 16) were prepared in order to give a direct comparison with the 1-methylheptyl esters discussed in § 2.3.1. In this series the polarity

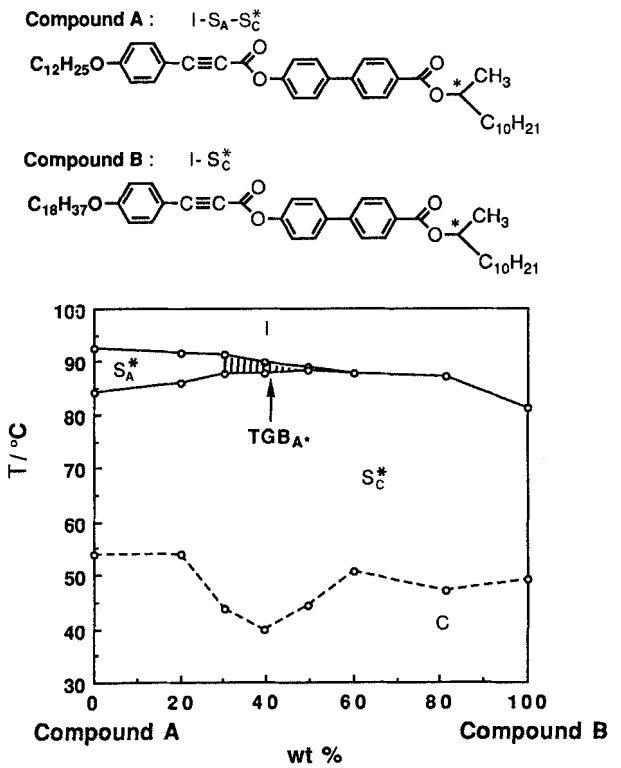

Figure 15. Binary phase diagram for mixtures (wt%) of (*S*)-1-methylundecyl 4′-(4″-*n*-dodecyloxyphenylpropioloyloxy)biphenyl-4-carboxylate and (*S*)-1-methylundecyl 4′-(4″-*n*-octadecyloxyphenylpropioloyloxy)biphenyl-4-carboxylate.

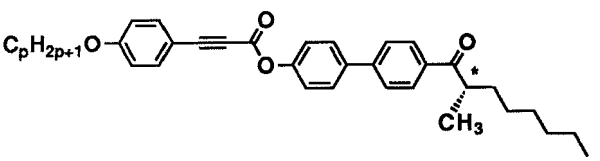

Figure 16. (*S*)-4-(2′-methyloctanoyl)biphenyl 4-*n*-alkoxyphenylpropiolates (2M8B*p*OPPs).

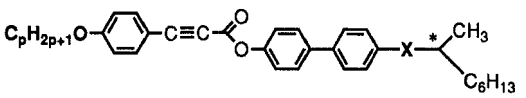

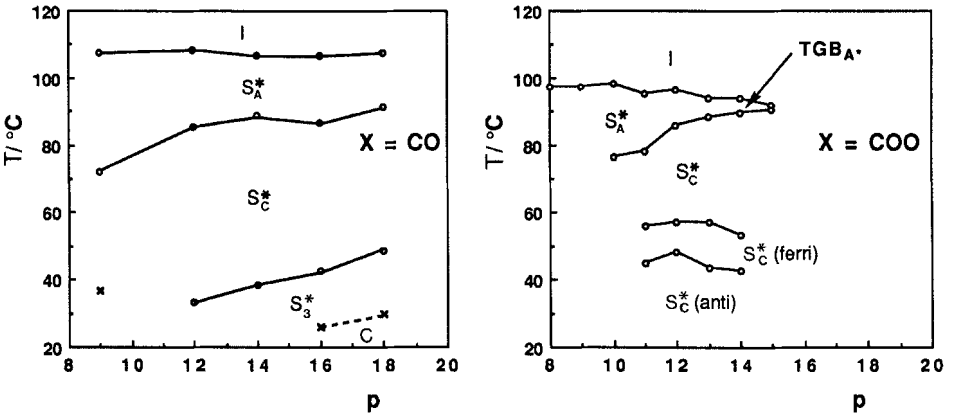

Figure 17. Transition temperatures for the (*S*)-4-(2′-methyloctanoyl)biphenylyl 4-*n*-alkoxyphenylpropiolates (2M8B*p*OPPs) plotted as a function of increasing terminal *n*-alkoxy chain length (*p*). The results are compared with those for the equivalent esters.

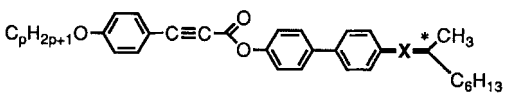

A: X = CO

B: X = COO

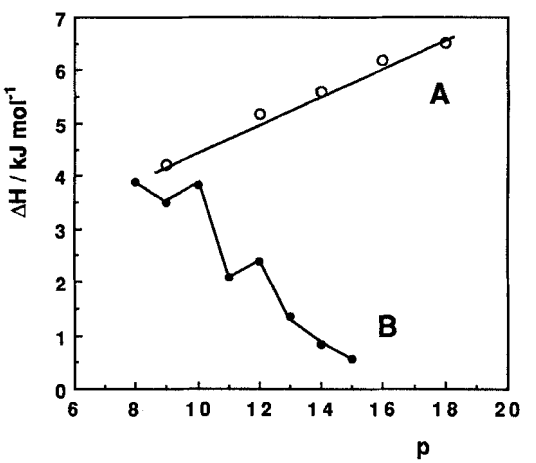

Figure 18. Comparison of the clearing point enthalpies (kJ mol^{-1}) for the carbonyl and ester series versus alkyl chain length, *p*.

of the linking group is increased over that of the ester equivalent, along with an increased ability to form hydrogen bonds. As a consequence, the molecules are expected to form stronger associations in the carbonyl series with respect to the esters.

Figure 17 shows a comparison of the transition temperatures for the carbonyl and ester series. The clearing transitions for the carbonyl series are higher than those for the ester equivalents, and hence the carbonyl group appears to improve the liquid crystal nature of the compounds. The carbonyl function also appears to stabilize smectic A* phases at slight expense to smectic C* phases. As a consequence, the smectic A* phase is never eclipsed by the smectic C* phase, and therefore no twist grain boundary phases are found in this series. This result is borne out by examination of the clearing enthalpies as a function of terminal *n*-alkoxy chain length, as shown in figure 18. This graphical comparison shows that the clearing enthalpies of the carbonyl series rise as the terminal aliphatic chain length is increased, whereas the converse is the case for the ester equivalents. This indicates that the layer structure in the carbonyl series is much more stable in comparison to the esters. These results are again in agreement with de Gennes' theory for the formation of defect stabilized phases. Furthermore, differential scanning calorimetry shows no liquid–liquid transitions detected as were for the esters.

2.3.5. *Effect of polarity at the chiral centre—the (S)-2-chloroalkyl esters*

The above sections describe how the liquid crystal properties change in the phenylpropiolates as the steric shape of the system is altered by varying the terminal substitutents; however, the lateral off-axis group at the chiral centre was in all cases a methyl substituent. In the following study [29]; the liquid crystal properties of the phenylpropiolates were evaluated as a function of changing polarity at the chiral centre incurred by the exchange of the methyl substituent for a halogen atom. Initial studies were carried out on the (*S*)-2-chloroalkyl 4′-(4″-*n*-nonyloxyphenylpropioloyloxy)-biphenyl-4-carboxylates (2Cl*q*9OPPBCs) (see figure 19).

The phase transition temperatures for a variety of members of the series are shown in figure 20. Unlike the series that carry a lateral methyl substituent, the chloro materials exhibit cholesteric phases as well as smectic phases. With increasing alkyl chain length the clearing points from the blue phases and the cholesteric phase to the isotropic liquid fall in value; however, the cholesteric to smectic A* transition temperatures rise, as do the values for the smectic A* to smectic C* phase change. For each member, the transition from the cholesteric to smectic A* phase is mediated by the formation of a twist grain boundary smectic A* phase. These materials are, therefore, examples of compounds that show behaviour described by the theory of Renn and Lubensky for the formation of a defect stabilized phase at the cholesteric to smectic A* transition. It is interesting to note that these materials also exhibit the closely related blue phases in addition to TGB phases. As with the methyl series, the temperature range of the TGB phase rises then falls as the series is ascended. Thus, the chirality increases to the point where it starts to become diluted by the length of the peripheral alkyl chain.

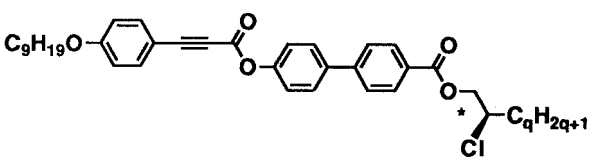

Figure 19. (*S*)-2-chloroalkyl 4′-(4″-*n*-nonyloxyphenylpropioloyloxy)biphenyl-4-carboxylates (2Cl*q*9OPPBCs).

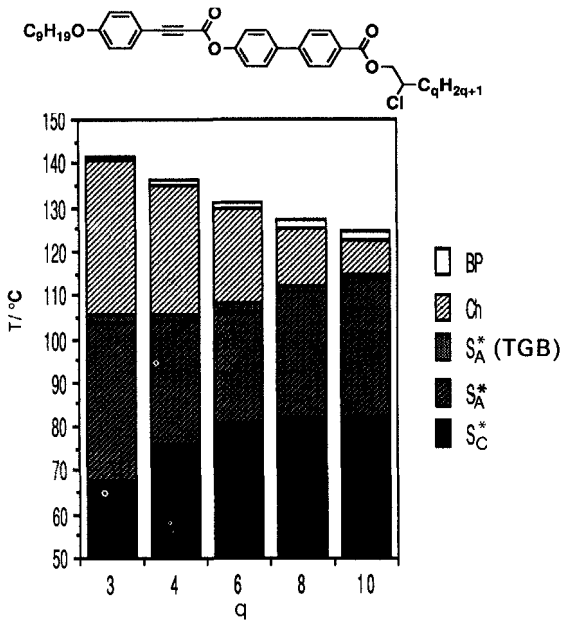

Figure 20. The transition temperatures of some (*S*)-2-chloroalkyl 4′-(4″-*n*-nonyloxyphenylpropioloyloxy)biphenyl-4-carboxylates (2Cl*q*9OPPBCs) shown as a function of alkyl chain length (*q*).

The degree and position of methyl branching in the peripheral alkyl chain of the chiral halide was also examined [29] as a function of a constant *n*-alkoxy chain appended to the phenylpropiolate portion of the system. The results for this series of compounds are shown schematically in figure 21. As with the preceding materials, these esters exhibit blue phases, cholesteric phases, and TGB_{A*}, smectic A* and smectic C* phases. At short terminal chain lengths no TGB phases are observed, but as the peripheral aliphatic chain is extended, TGB_{A*} phases appear, and their temperature ranges increase with increased branching and chain length. One interesting comparison can be drawn from the derivatives that have sequential chiral centres obtained by synthesis from isoleucine (*S*,*S*) and *allo*-isoleucine (*S*,*R*). For the material with opposite spatial configurations of the two sequential chiral centres in the terminal chain (*allo*-isoleucine), a wider temperature range for the TGB_{A*} phase was obtained in comparison to the material that has two chiral centres with the same configuration (isoleucine).

The effect that changing the halogen atom has on the liquid crystal properties was also investigated. The halogen was systematically changed from fluorine to chlorine to bromine for one particular phenylpropiolate, the results for which are shown in table 5. The results show that by increasing the size and the polarizability of the halogen atom, the smectic A* temperature range increases, thereby stabilizing the layer structure and depressing the formation of TGB smectic A* phases. It is also possible that for the bromide the off-axis size of the atom is so large that the chiral centre cannot rotate easily about the long axis of the molecule (see figure 22). This may have the effect of positioning the bromine atom on the opposite side of the long axis of the carbonyl moiety. This would, in principle, reduce the steric hindrance between neighbouring molecules, thereby reducing the molecular chirality of the system and consequently suppressing TGB phases.

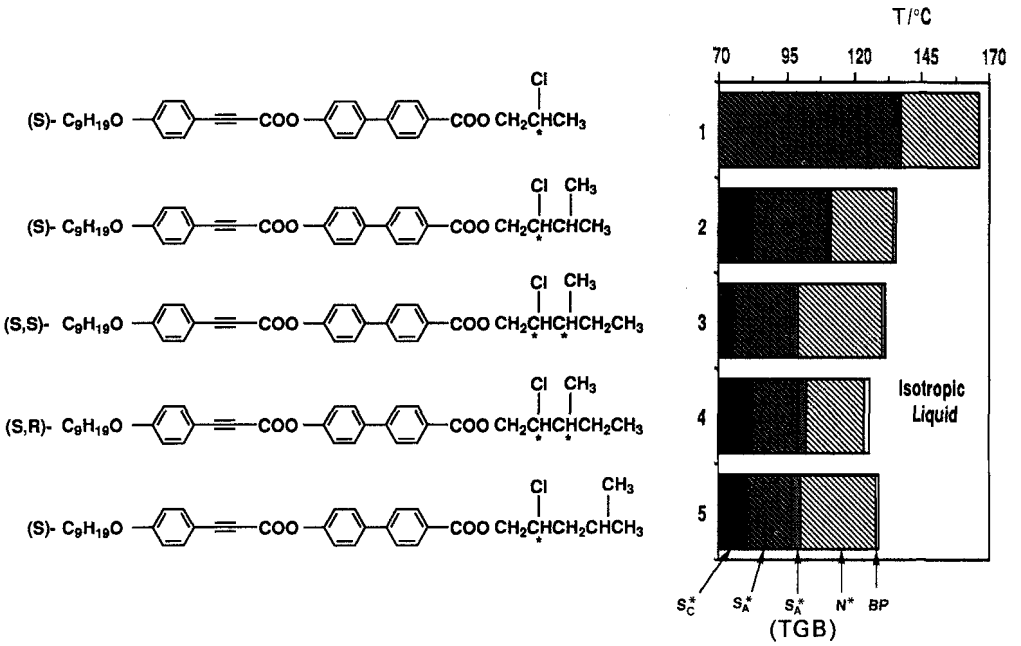

Figure 21. The effects of branching in the terminal aliphatic chain on the liquid-crystalline transitions of the (*S*)-2-chloro-methylalkyl 4′-(4″-*n*-nonyloxyphenylpropioloyloxy)biphenyl-4-carboxylates.

Table 5. The effect of halogeno-substitution at the chiral centre in a variety of 2-halogeno-methylalkyl 4′-(4″-*n*-nonyloxyphenylpropioloyloxy)biphenyl-4-carboxylates.

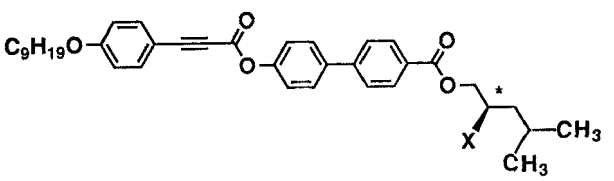

X	T_{ICh}/°C	$T_{ChS_A^*}$ or $T_{ChTGB_A^*}$/°C	$T_{TGB_A^*S_A}$/°C	$T_{S_A^*S_C^*}$/°C
F	143·0	114·0	112·0	96·0
Cl	129·4	100·4	96·8	79·9
Br	123·6	99·4	—	72·3

Increasing S_A^* range

2.3.6. *The effect of optical purity and novel liquid phases*

It is possible for many of the materials, reported in the sections above, to prepare the racemic modification by synthetic procedures or by simply mixing the (*R*) and (*S*) enantiomers. The very first study [15] of this nature was for 1-methylheptyl 4′-(4″-*n*-tetradecyloxyphenylpropioloyloxy)biphenyl-4-carboxylate (1M714OPPBC) where the racemic modification and the two enantiomers were individually prepared by synthetic procedures. This investigation was proposed in order to confirm that the chiral *n*-tetradecyloxy compounds did indeed exhibit smectic phases and not cholesteric phases (as they were the first low molar mass materials to exhibit TGB

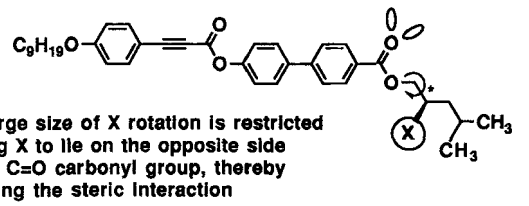

Figure 22. Schematic representation of the restricted rotation in the halogeno-substituted phenylpropiolates.

Table 6. Effect of the degree of optical purity on the liquid crystal transition temperatures of 1-methylheptyl 4″-(4′-*n*-tetradecyloxyphenylpropioloyloxy)biphenyl-4-carboxylate on the heating cycle. The transition enthalpies are in brackets.

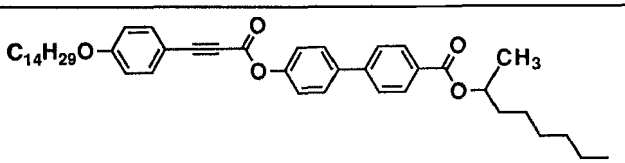

	T_{IS_A} or $T_{IS_A^*}$/°C	$T_{S_AS_C}$ or $T_{S_AS_C^*}$/°C	$T_{S_C^*S_3}$/°C	$T_{S_3S_4}$/°C	T_{Rec}/°C
(*R*) or (*S*) Isomer	93·8	89·7	49·5	38·3	78·0
	[0·84]	[0·11]	—	—	[19·8]
Racemate (±)	97·7	90·3	—	—	69·5
	[3·46]	[0·14]	—	—	[19·2]

[ ] ΔH values in kJ mol^{-1}.

phases, the initial phase classification was difficult). The remarkable results obtained for the phase behaviour of these three materials are shown in table 6 and the differential scanning thermograms in figure 23. It can be seen from the table that the clearing point temperature falls by about 4°C when the optical purity is raised from zero for the racemate to about 98 per cent for either of the enantiomers. (Both commercially available (*S*) and (*R*)-2-octanols are found to have optical purities in this range.) On the other hand the TGB_{A^*} to smectic C* transition temperatures remain relatively insensitive to enantiomeric excess. Moreover, the chiral compounds are also found to exhibit ferrielectric and antiferroelectric phases on cooling the smectic C* phase, whereas for the racemate these transitions are absent. Surprisingly the differential scanning thermograms show that the enthalpy for the clearing point transition is much larger for the racemate than for either enantiomer. In fact a further transition was detected in the isotropic liquid region above the clearing point for the enantiomers. The maximum of this transition is found to be at approximately the same temperature as the clearing point for the smectic A to liquid transition in the racemate, and furthermore the total enthalpy for the clearing transition for either enantiomer (TGB_{A^*} to isotropic liquid plus the liquid–liquid transition) is approximately equal to that for the smectic A to isotropic transition for the racemate. This suggests that the clearing transition for the optically active isomers occurs *via* a two stage process. The shift to lower temperatures for the liquid crystal to liquid transition as a function of optical purity was theoretically predicted by de Gennes for defect stabilized phases.

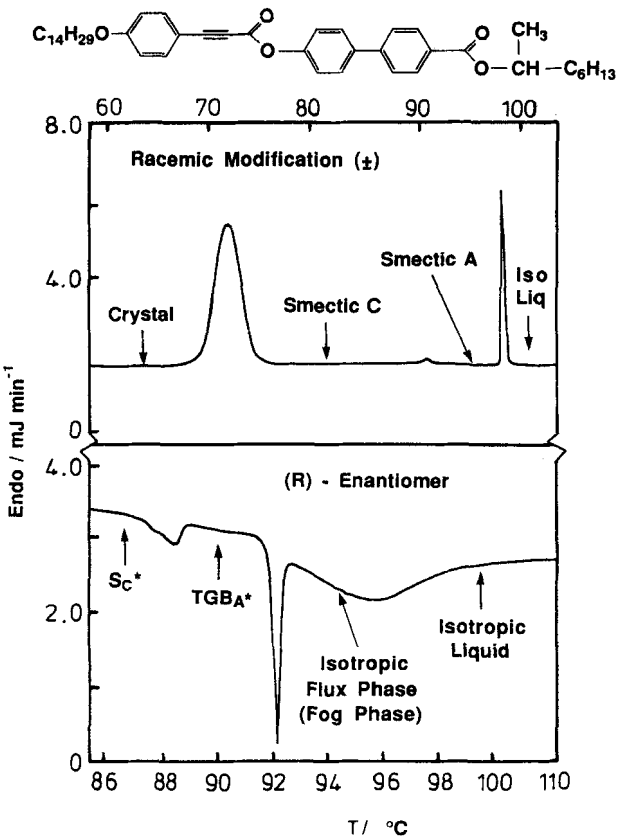

Figure 23. Differential scanning calorimetry traces for the heating cycle of the racemate and the cooling cycle of the (*R*)-enantiomer (heating and cooling rates 2°C min^{-1}).

The transitions in the isotropic liquid are similar to those discussed in §2.3.3. and are indicative of a two stage process occurring. This may well take the form of either the cores of the defects melting first to give a disordered liquid-like smectic A phase where the layers exist over very short distances, i.e. a cybotactic smectic A phase in the liquid, or where the cores of the defects remain once the intermediary smectic A regions have melted. In the latter case an entangled or disentangled flux phase is obtained. This behaviour is similar in nature to that found for the fog phase in blue phase transitions.

2.3.7. *The effect of ring substituents—the TGB_{C^*} phase*

The homologous (*R*)- and (*S*)-1-methylheptyl 4′-(3″-fluoro-4″-*n*-tetradecyloxyphenylpropioloyloxy)biphenyl-4-carboxylates were found to exhibit even more bizarre behaviour in relation to that shown by the unsubstituted analogues (1M714OPPBCs) [30]. The racemic modification of these enantiomers exhibits smectic A and smectic C phases, but for each enantiomer the smectic A* to isotropic liquid crystal transition is suppressed below that for the smectic A* to smectic C* phase change. Thus, the enantiomers exhibit direct isotropic liquid to smectic C* transitions. The transition temperatures for these materials are shown in table 7, and the differential scanning thermograms in figure 24. The DSC traces are quite unusual because the

Table 7. Transition temperatures for the (*R*) and (*S*) enantiomers, and the racemic modification of 1-methylheptyl 4′-(3″-fluoro-4″-*n*-tetradecyloxyphenylpropioloyloxy)biphenyl-4-carboxylate.

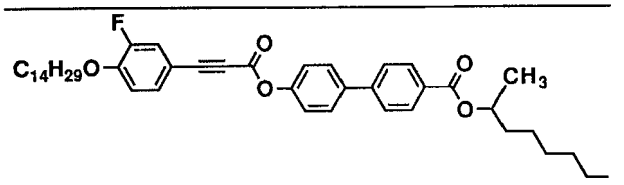

Racemate (±): I 81·5°C S_A 79·3°C S_C 44·8°C C	
(*R*) isomer: I 75·3°C S_C^* 49·6°C C	No S_A phase
(*S*) isomer: I 75·5°C S_C^* 62·7°C C	

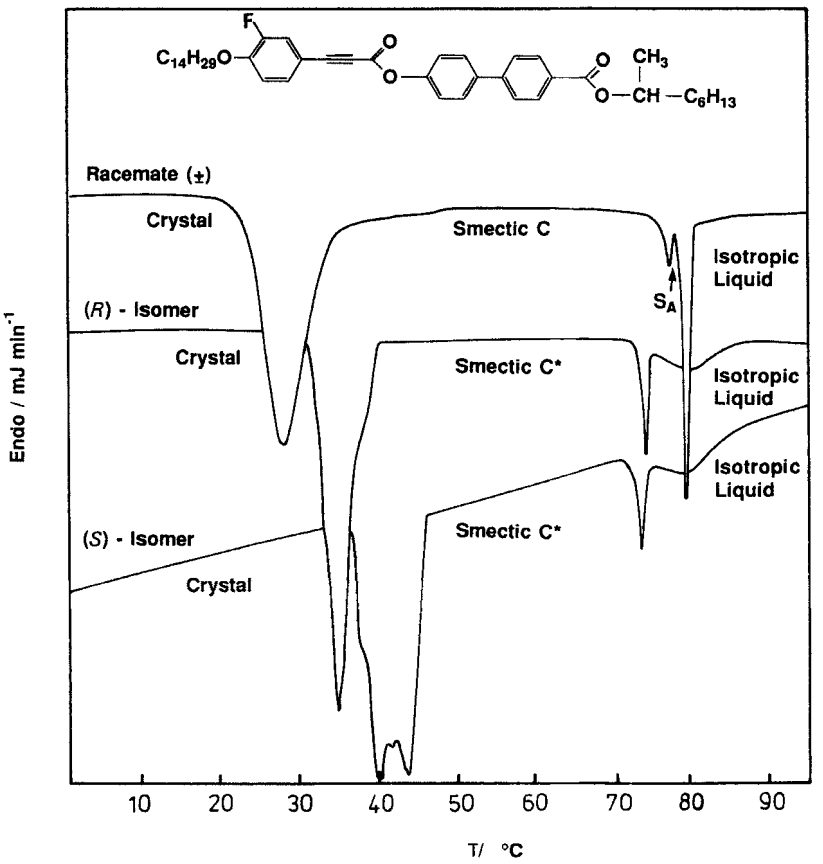

Figure 24. DSC cooling traces for the 1-methylheptyl 4′-(3″-fluoro-4″-*n*-tetradecyloxyphenylpropioloyloxy)biphenyl-4-carboxylates (cooling rate 2°C min^{-1}).

isotropic liquid to smectic A transition for the racemate is replaced by a liquid–liquid transition in the enantiomers. The cooling cycles show how the peak for the isotropic liquid to smectic A transition overlays perfectly the liquid–liquid transitions for the enantiomers. Furthermore, the smectic A to smectic C transition for the racemate appears to be more first order in nature than is usually expected. Mixture studies between the two enantiomers also produced interesting examples of phase behaviour. In the phase diagram, a smectic A phase appears in the centre of the concentration range, i.e. for the racemate. When either enantiomer is present in proportions around 60 per cent by weight, a TGB_{A^*} phase appears between the liquid state and the normal A* phase. A slight increase in the concentration of the enantiomer in excess reveals a transition to a phase that we believe is a TGB_{C^*} phase. The phase exhibits a normal smectic C* schlieren texture and has a helical structure. Cooling this phase results in a transition to a normal smectic C* phase which is iridescent and has its helical axis at right angles to that of the preceding phase, hence our belief that the intermediary phase is a twist grain boundary smectic C* phase [30]. At high concentrations of either of the enantiomers in the binary mixture a liquid–liquid transition is again detected by DSC. Thus, this complicated mixture system serves to exemplify some of the unusual effects that chirality has in self-ordering systems.

2.4. *Antiferroelectric and ferrielectric phases*

In the process of investigating how molecular chirality changes with the size, shape and polarity of the lateral group at the chiral centre, we also investigated systems where the terminal chiral moiety essentially carries two aliphatic chains [28], as shown in figure 25. For this liquid crystal system, we were able independently to vary the length of the two terminal chains (q and r) at the chiral centre and examine how this affected the chiral properties of the mesophases formed. In particular, it could be imagined that, as the terminal chiral moiety becomes more fork-shaped in structure, the chirality of the phase would be increased due to rotational damping of the motion of the chiral centres about the long axes of the molecules. Similarly the biaxiality of the material might also be expected to increase as the lengths of the two terminal chains (q and r) are increased. The transition temperatures for a variety of these esters are shown in table 4. The results show that when the lateral aliphatic substituent is increased in length (increasing value of r for a constant value of q), then antiferroelectric phases are favoured over ferroelectric and ferrielectric phases. For example, for $q=9$ and $r=3$ a direct smectic A* to antiferroelectric smectic C* transition takes place, with the ferroelectric phase being totally eclipsed. This trend is clearly shown in the comparison of the transition temperatures for the series of compounds where $p=9$, $q=6$ and r is varied from 1 to 3. The clearing temperatures fall, as does that for the smectic A* to smectic C* transition, which is eventually replaced by a transition to the antiferro-phase, see figure 26. Similarly TGB phases are also suppressed by increasing the length of the lateral substituent. When the two terminal chain lengths reach the same value

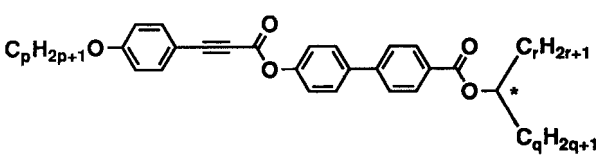

Figure 25. (*R*)- and (*S*)-alkylalkyl 4′-(4″-*n*-alkoxyphenylpropioloyloxy)biphenyl-4-carboxylates.

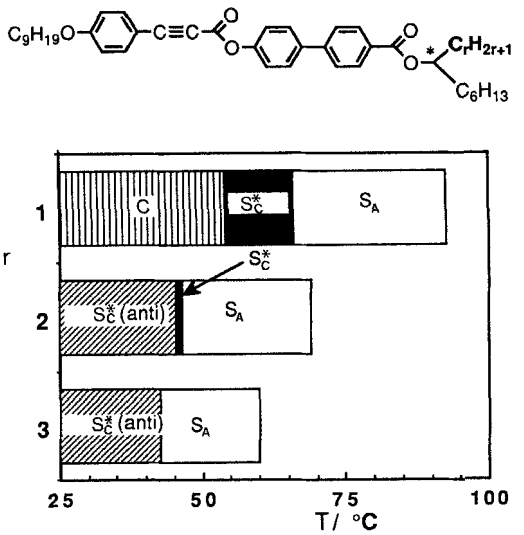

Figure 26. Transition temperatures plotted as a function of alkyl chain length (r) in the alkylheptyl 4′-(4″-*n*-nonyloxyphenylpropioloyloxy)biphenyl-4-carboxylates.

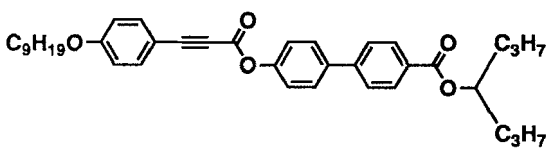

Figure 27. Structure and transition temperatures for the achiral compound 1-propylbutyl 4′-(4″-*n*-nonyloxyphenylpropioloyloxy)biphenyl-4-carboxylate.

($p=9, r=q=3$) then the material has no chirality, but it still exhibits an antiferroelectric-like phase on cooling from the smectic A phase [31] (see figure 27). Thus, this is the first example of an achiral antiferro-phase, indicating that chirality does not necessarily stabilize the formation of ferrielectric and antiferroelectric structures, but rather that the structure may be stabilized by the biaxial nature of the molecular structure. This material therefore may form part of a host system for preparing eutectic mixtures of antiferroelectric materials for applications in displays.

2.5. *Twist inversions in cholesteric phases*

The propiolate ester (*S*)-2-chloropropyl 4′(4″-*n*-nonyloxyphenyl-propioloyloxy)biphenyl-4-carboxylate (9O2Cl3T) [32] (figure 28) was found to have the following phase sequence and transition temperatures:

mp 102·6°C I 166·0°C N* 137·0°C S_{A^*} 62·0°C C.

On cooling this material between untreated glass slides, the cholesteric phase forms from the isotropic liquid to give a characteristic fingerprint texture. As the temperature is reduced the pitch of the cholesteric phase begins to increase. This is clearly seen as the fingerprints associated with the pitch of the phase increase in breadth. At about 150°C, regions of pseudo-homeotropic texture become apparent as the cholesteric phase splits

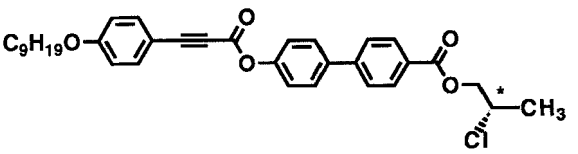

Figure 28. Structure and transition temperatures of (*S*)-2-chloropropyl 4′-(4″-*n*-nonyloxyphenylpropioloyloxy)biphenyl-4-carboxylate (9O2Cl3T).

up into fingers which then gradually reduce in size. On further cooling the whole texture of the cholesteric phase disappears giving way to the homeotropic texture of a nematic phase. This texture is found to flash, when subjected to mechanical stress, in a way characteristic of the nematic phase. Further cooling produces another cholesteric phase at approximately 141°C, which can be shown to have the opposite twist sense to the higher temperature cholesteric phase. The formation of this lower temperature cholesteric phase is promptly followed by a normal transition to the smectic A* phase at 137°C.

Conclusive establishment that the two cholesteric phases observed have opposite twist senses was made from contact preparations. Furthermore, the pitch of the cholesteric phase of the material was measured and shown to diverge at about 142°C. Interestingly the reciprocal of the pitch is found to vary linearly with temperature and therefore the inversion point for the helical structure can be determined relatively accurately (to within 1°C).

This extraordinary behaviour is thought to occur through the competition of different conformer species, as postulated for other similar inversion phenomena. The conformer species are thought to have different helical preferences and twisting powers, and the species are believed to interconvert between one another at a relatively rapid rate. Thus, at any one temperature there will be a distribution of conformers leading to an overall helical structure with a pitch length averaged over the number of conformers. As the temperature is altered the distribution of conformers changes, and accordingly the pitch and handedness of the helical structure may also change. For conformers that are in competition, it is therefore quite possible that the helical structure might invert through a non-helical nematic phase. A schematic representation of the various conformer species present for the 2-chloro compound is shown in figure 29. Thus, we can define three extreme conformational structures produced by rotations about the C_1–C_2 bond (for A, B and C in figure 29) for which there will be differing dipole directions and different steric structures. In conformer C, the sizes of the chloro and methyl substituents are rather similar and they are positioned on equivalent, but opposite sides, of the long axis. Thus, it might be expected that the steric effects of the two off-axis substituents in this conformer could compensate for one another. However, this is not the case for conformers A and B where either the chloro or the methyl substituent is located on the side of the long axis of the molecule. In these two situations, therefore, it is quite possible that the extreme conformers A and B could produce opposing helical twist senses, based on steric effects. For example, the projections of the two species show that in conformer A, where the terminal methyl group is included in the long axis of the molecule, chlorine points into the page, whereas for the reversed situation, conformer B, with chlorine in the long axis, the methyl group now points out of the page. If the helix direction is sterically driven, then its twist sense will be dependent on the relative concentrations of such conformers in the pure material, and as noted above it is expected that the twist senses of conformers A and B

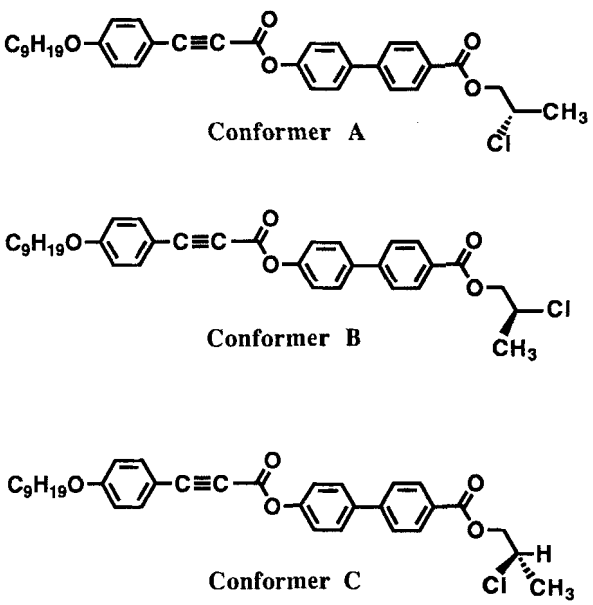

Figure 29. Various conformer species for (*S*)-2-chloropropyl 4′-(4″-*n*-nonyloxyphenylpropioloyloxy)biphenyl-4-carboxylate (9O2Cl3T).

will oppose one another causing a twist inversion. However, the point at which the pitch of the cholesteric helix diverges need not necessarily occur at a 50:50 concentration of the two species A and B, as the two conformers will have different twisting powers. For example, if conformer A induces a very short pitch whereas conformer B induces a very long pitch, the inversion point will occur at a concentration of conformer A that is much less than 50 per cent.

A similar situation can also be found for some of the smectic C* phases exhibited by the chloro-substituted esters. However, in these materials the twist inversion in the helical smectic C* phase does not appear to go through a totally unwound state. This is a somewhat confusing result and therefore these materials are not discussed in detail here. However, they provide further examples of unusual phase behaviour in phenylpropiolates.

3. Summary

We have demonstrated that phenylpropiolates are capable of exhibiting the following phase behaviour.

(i) Isotropic to TGB_{A*} transitions were found in the 1-methylheptyl derivatives.
(ii) Isotropic to cholesteric to TGB_{A*} to smectic A* phase sequences were found in the 2-chloro-alkyl compounds.
(iii) Ferrielectric and antiferroelectric phases appear in chiral materials, but not in their racemic modifications.
(iv) A non-chiral antiferroelectric material was prepared and evaluated.
(v) Extension of the branch at the chiral centre suppresses ferroelectric and TGB phases, but promotes antiferroelectric properties.

(vi) The layer structure in some phenylpropiolate esters was found to be weak and therefore TGB phases were formed in contrast to their carbonyl analogues where the layer ordering was found to be stronger and no such phases were found.

(vii) Increasing the peripheral chain on the external side of the chiral centre increases the molecular chirality, which reaches a plateau and then falls due to dilution effects of chain length. Thus the incidence of TGB phases increases and then decreases as the chain is lengthened.

(viii) TGB_{C*} phases are believed to occur in phases diagrams.

(ix) TGB_{A*} phases appear in mixtures where the temperature range of the normal smectic A* phase is reduced.

(x) Twist inversions occur in both the cholesteric and the smectic C* phases of some of the chiral chloro-compounds; these inversions are thought to be due to competition between various conformer species.

Overall therefore we can sum up some of the relationships developed between molecular structure, molecular chirality and phase behaviour in the form of a figure (figure 30). Although not specifically discussed in this article some other issues concerning chiral properties such as the magnitude of the polarization in ferroelectric phases and the pitch length in helical phases are included in the figure. Many physical studies have been performed on phenylpropiolates, the details of which are two extensive to report here, however, figure 30 does include some of the property–structure correlations that we have developed from studying these materials. Thus, in this article we have been only able to give a brief overview of the many interesting effects produced by molecular chirality in organized systems. More detailed reports on the nature and results of this work are already published or are in the press.

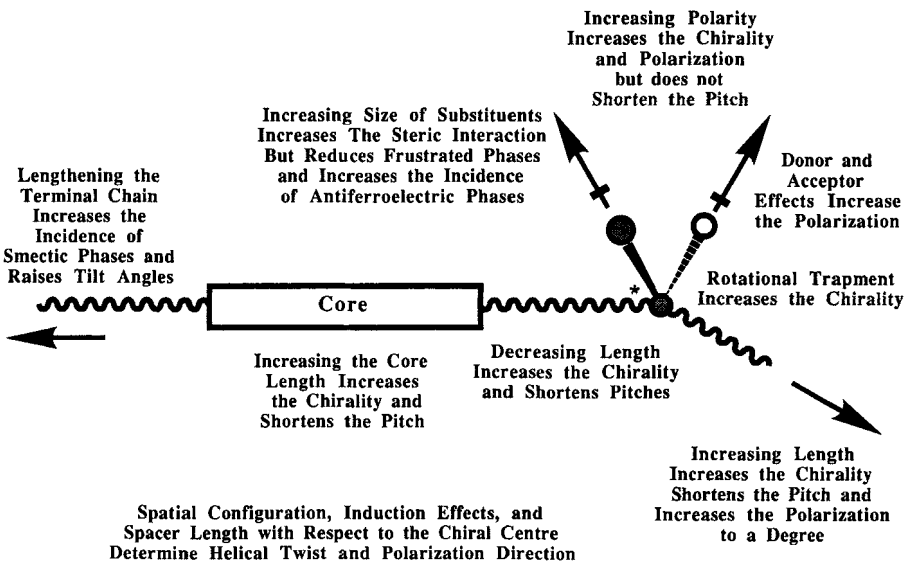

Figure 30. Schematic representation of the relationship between physical properties and molecular structure in chiral liquid crystal materials.

We are grateful to the SERC (UK), SERC/MoD and Nippon Mining Co Ltd for financial support, and to Dr R. Pindak, Dr J. S. Patel, Dr M. A. Waugh, Miss E. Chin, Miss S. M. Stein, and Professors H. Fukuda and H. Takezoe for useful discussions. We also wish to thank Nippon Mining Co. Ltd. for supplying many starting materials, and Mr R. Knight, Mr A. R. Roberts, Mrs B. Worthington, and Dr D. F. Ewing for spectroscopic analyses of the final products and synthetic intermediates.

References

[1] Reinitzer, F., 1888, *Mh. Chem.*, **9**, 421. Lehmann, O. Z., 1889, *Z. phys. Chem.*, **4**, 462.
[2] Grabmaier, J. G., 1975, *Applications of Liquid Crystals*, edited by G. Meier, E. Sackmann, and J. G. Grabmaier (Springer-Verlag), p. 83.
[3] Coates, D., and Gray, G. W., 1973, *Physics Lett.* A, **45**, 115.
[4] Crooker, P. P., 1989, *Liq. Crystals*, **5**, 751.
[5] Meyer, R. B., 1976, *Molec. Crystals liq. Crystals*, **40**, 74.
[6] Clark, N. A., and Lagerwall, S. T., 1980, *Appl. Phys. Lett.*, **36**, 899.
[7] Meyer, R. B., Liebert, L., Strezlecki, L., and Keller, P., 1975, *J. Phys. Lett., Paris*, **36**, L69.
[8] Garoff, S., and Meyer, R. B., 1977, *Phys. Rev. Lett.*, **38**, 848.
[9] Bahr, Ch., and Heppke, G., 1987, *Molec. Crystals liq. Crystals*, **148**, 29.
[10] Chandani, A. D. L., Gorecka, E., Ouchi, Y., Takezoe, H., and Fukuda, A., 1989, *Jap. J. appl. Phys.*, **28**, L1265.
[11] Yamawaki, M., Yamada, Y., Yamamoto, N., Mori, K., Hayashi, H., Suzuki, Y., Negi, Y. S., Hagiwara, T., Kawamura, I., Orihara, H., and Ishibashi, Y., 1989, *Proceedings 9th International Display Research Conference (Japan Display 89)*, p. 26.
[12] Chandani, A. D. L., Hagiwara, T., Suzuki, Y., Ouchi, Y., Takezoe, H., and Fukuda, A., 1988, *Jap. J. appl. Phys.*, **27**, L729.
[13] de Gennes, P. G., 1972, *Solid St. Commun.*, **10**, 753.
[14] Renn, S. R., and Lubensky, T. C., 1988, *Phys. Rev.* A, **38**, 2132.
[15] Goodby, J. W., Waugh, M. A., Stein, S. M., Chin, E., Pindak, R., and Patel, J. S., 1989, *J. Am. chem. Soc.*, **111**, 8119.
[16] Srajer, G., Pindak, R., Waugh, M. A., Goodby, J. W., and Patel, J. S., 1990, *Phys. Rev. Lett.*, **64**, 1545.
[17] Taborek, P., Goodby, J. W., and Cladis, P. E., 1989, *Molec. Crystals liq. Crystals*, **4**, 21.
[18] Freidzon, Ya. S., Tropsha, Ye. G., Tsukruk, V. V., Shilov, V. V., Shibaev, V. P., and Lipatov, Yu. S., 1987, *J. Polym. Chem. (U.S.S.R.)*, **29**, 1371.
[19] Goodby, J. W., 1991, *J. mater. Chem.*, **1**, 307.
[20] Goodby, J. W., Patel, J. S., and Chin, E., 1991, *J. mater. Chem.*, **2**, 197.
[21] Nishiyama, I., and Goodby, J. W., 1992, unpublished results.
[22] Corey, E. J., and Fuchs, P. L., 1972, *Tetrahed. Lett.*, 3769.
[23] Mitsunobu, O., 1981, *Synthesis*, 1.
[24] Chin, E., and Goodby, J. W., 1986, *Molec. liq. Crystals*, **141**, 311.
[25] Hassner, A., and Alexanian, V., 1978, *Tetrahed Lett.*, 4475; Kim, S., Lee, J. I., and Ko, Y. K., 1978, *Tetrahed. Lett.*, 4943.
[26] Ihn, K. J., Zasadzinski, J. A. N., Pindak, R., Slaney, A. J., and Goodby, J. W., 1992, *Science*, **258**, 275.
[27] Waugh, M. A., Stein, S. M., Chin, E., and Goodby, J. W., 1992, *Liq. Crystals*, **11**, 135.
[28] Nishiyama, I., 1992, Ph.D. Thesis, University of Hull.
[29] Slaney, A. J., and Goodby, J. W., 1992, *Liq. Crystals*, **9**, 849; Slaney, A. J., 1992, Ph.D. Thesis, University of Hull.
[30] Booth, C. J., Goodby, J. W., and Toyne, to be published.
[31] Nishiyama, I., and Goodby, J. W., 1992, *J. mater. Chem.*, **2**, 1015.
[32] Slaney, A. J., Nishiyama, I., Styring, P., and Goodby, J. W., 1992, *J. mater. Chem.*, **2**, 805.